Electronic density response of liquid water using time-dependent density functional theory

I. Tavernelli
Ecole Polytechnique Fédérale de Lausanne, Institut des Sciences et Ingénierie Chimiques, EPFL-BCH, CH-1015 Lausanne, Switzerland
(Received 14 December 2005; published 28 March 2006)

Time-dependent density functional theory is used to compute the linear response of a sample made of 32 periodically replicated water molecules. We study the relaxation effects following two different perturbation schemes, namely a point charge disturbance and a sudden switch of an external electric field. The approach, which is based on the real-time propagation of the time-dependent Kohn-Sham equations, is used for the computation of the response and dielectric functions of configurations equilibrated at 298 K. A real-time imaging of the density disturbance with a time resolution of 1.2 attoseconds is obtained.

DOI: 10.1103/PhysRevB.73.094204 PACS number(s): 31.15.Ew, 71.15.Mb, 78.20.Bh

I. INTRODUCTION

The equilibrium structure of liquid water and in particular its hydrogen bond network is still a subject of major debate among experimental and theoretical research groups.[1–3] However, less is known about the predictions of first principle calculations on the electronic response properties of water. Even though experimental results are available,[4–6] the computation of the electronic response properties of liquid water (with and without the presence of ions or solute molecules) still represents a challenging theoretical problem.[7–10] The knowledge of the microscopic perturbations induced by a sudden change in the charge distribution (for instance after excitation of a chromophore) on the electronic structure of the solvent has many important implications in physics, chemistry, and biology. A number of studies have focused on the characterization of the disturbance induced by an excess electron in solution.[11,12] In this work we use time-dependent density functional theory (TDDFT) to investigate the microscopic nature of the electronic response in liquid water by means of an external perturbation induced by a charge density disturbance $\rho_{\text{ext}}(\mathbf{r},t)$, which has designed spatial and temporal dependences, and an external electric field.

When an inhomogeneity in the electronic structure is produced, the electrons put themselves into motion in order to reestablish neutrality (screening), and as electrons possess inertia, they acquire an oscillatory motion around the equilibrium state. The collective movement of the electrons, called plasma oscillation or *plasmon*, is driven by the long range restoring force (Coulomb attraction) between the constituents of opposite charge. In the following we assume a linear dependence between the induced charge density, $\rho_{\text{ind}}(\mathbf{r},t)=\rho(\mathbf{r},t)-\rho_0(\mathbf{r})$, and the perturbation, which is taken sufficiently weak. (Here ρ refers to the electron density at a time t after the perturbation and ρ_0 is the unperturbed density).

If the functional dependence between the excitation and the response is analytic, the most general linear relation is

$$\rho_{\text{ind}}(\mathbf{r},t)=\int dt' \int d\mathbf{r}'\chi(\mathbf{r},\mathbf{r}',t,t')\rho_{\text{ext}}(\mathbf{r}',t'), \qquad (1)$$

where $\chi(\mathbf{r},\mathbf{r}',t,t')$ is the time-retarded response function, with the property $\chi(\mathbf{r},\mathbf{r}',t,t')=0$, for $(t-t')<0$.[13] The total charge density displacement at time t is given by $\rho_{\text{tot}}(\mathbf{r},t)=\rho_{\text{ind}}(\mathbf{r},t)+\rho_{\text{ext}}(\mathbf{r},t)$ and is related linearly to the external density by the *dielectric function* $\epsilon(\mathbf{r},t)$. In the case of isotropic homogeneous systems it is often convenient to Fourier transform all quantities in both space and time to obtain the simple relation $\rho_{\text{ind}}(\mathbf{k},\omega)=\chi(\mathbf{k},\omega)\rho_{\text{ext}}(\mathbf{k},\omega)$ (using the same symbol in Fourier space for all functions). The relation between ε and χ assumes then the form, $\varepsilon(\mathbf{k},\omega)/\varepsilon_0=[\chi(\mathbf{k},\omega)+\mathbf{1}]^{-1}$. However, due to the inhomogeneity of our microscopic sample, it is often convenient for us to keep the formalism in the real space formulation. In the case of a localized instantaneous perturbing charge density pulse[6] issued at time t_0, $\rho_{\text{ext}}(\mathbf{r},t)=\delta(\mathbf{r}-\mathbf{r}_0,t-t_0)$, the induced charge density corresponds to the response function $\chi(\mathbf{r}-\mathbf{r}_0,t-t_0)=\tilde{\chi}(\mathbf{r},t)$, which becomes therefore accessible to our calculations.

As a second perturbation scheme, we study the electric field oscillation induced by a short duration external electric field $\mathbf{E}_{\text{ext}}(t)=-A_0\hat{z}\delta(t)$, which contains all frequencies. Evaluation of the effective (or polarization) electric field, $\mathbf{E}(t)$, in the sample allows the computation of the dielectric function, $\varepsilon(\omega)$, according to[14]

$$1-\frac{1}{\varepsilon(\omega)}=\frac{1}{A_0}\int_{0^+}^{\infty} e^{i\omega t-\eta t}E_z(t)dt, \qquad (2)$$

where η is a small quantity to establish the imaginary part of the response[14] and E_z is the intensity of the field polarized along the z axis.

II. METHODS AND COMPUTATIONAL DETAILS

The generalization of density functional theory (DFT) to TDDFT[15] has become an important tool in the description of light-matter interaction in molecular[16,17] and condensed phase systems.[18] Possible applications range from calculations of spectra to the evaluation of properties like polarizability and hyperpolarizability,[19] and the study of photochemical reactions.[20] The formal justification of TDDFT was given by Runge and Gross.[15] The numerical solution of the corresponding time-dependent Kohn-Sham equations (TDKS) for an N-electron system

$$i\frac{\partial}{\partial t}\psi_k(\mathbf{r},t)=\left(-\frac{\nabla^2}{2}+v_{\mathrm{eff}}[\rho_t](\mathbf{r},t)\right)\psi_k(\mathbf{r},t) \tag{3}$$

with

$$v_{\mathrm{eff}}[\rho_t](\mathbf{r},t)=v_{\mathrm{ext}}(\mathbf{r},t)+\int\frac{\rho(\mathbf{r}',t)}{|\mathbf{r}-\mathbf{r}'|}d\mathbf{r}'+v_{xc}[\rho_t](\mathbf{r},t) \tag{4}$$

and the exchange-correlation potential given by

$$v_{xc}[\rho_t](\mathbf{r},t)=\frac{\delta\mathcal{A}_{xc}[\rho_t]}{\delta\rho(\mathbf{r},t)}, \tag{5}$$

can be obtained either perturbatively in the linear-response regime[17,21] or by direct integration in the time domain.[20,22,23] $\mathcal{A}_{xc}[\rho_t]$ in Eq. (5) is the exchange-correlation part of the action functional,[24] which depends in principle on the entire history of the density, $\rho(\mathbf{r},t)$, and on the initial Kohn-Sham orbitals, $\{\psi_k(\mathbf{r},t=0)\}$. The latter approach is particularly suited for our purposes, giving direct access to the time-dependent perturbed electronic density, $\rho(\mathbf{r},t)=\Sigma_{k=1}^{N}|\psi_k(\mathbf{r},t)|^2$.

In our calculations, the integration of the equations of motion was performed using the iterative scheme developed by Baer *et al.*[25] with a time step Δt of 1.21 attoseconds (as) combined with a two-step Runge-Kutta scheme to maintain order Δt^3 accuracy.[26] The liquid water sample was modeled by a periodically repeated cubic box of size L=9.86 Å containing 32 water molecules, which reproduces the density of liquid water at standard conditions. The long range electrostatic potential was computed using the standard Ewald summation scheme. All simulations were performed with the plane wave Kohn-Sham (KS) based DFT code CPMD.[27] Core electrons were replaced by pseudopotentials of the standard Troullier-Martins form.[28] The Kleinman-Bylander[29] integration scheme was used for both atom types, and the plane wave basis was truncated at an energy cutoff of 70 Ry. The exchange correlation energy was calculated using the GGA functional BLYP,[30,31] and the TDDFT calculations were performed within the so-called adiabatic approximation.[32] The atomic configurations used for this study were taken from an equilibration run performed with the Car-Parrinello MD algorithm,[33] a fictitious electronic mass of 500 a.u., and a time step of 0.1 fs. The temperature was set to 298 K using a Nosé-Hoover thermostat.[34] A perturbing external potential of the form of a short rectangular pulse generated by a charge of $1e$ was applied at time t_0 for a duration of 1.21 as . The electron density difference with the initial unperturbed density ρ_0, $\delta\rho(\mathbf{r},t)=-\rho_{\mathrm{ind}}(\mathbf{r},t)=\rho_0(\mathbf{r})-\rho(\mathbf{r},t)$, was sampled at time steps of 1.21 as for fixed nuclear geometries. For analysis, the cell volume was partitioned into Voronoi polyhedra centered at each water molecule and the corresponding electron density oscillation was monitored separately for each molecule.

A real-space description of polarization effects and electric response induced by a uniform (macroscopic) external electric field in a periodically replicated sample was recently proposed.[14] Since the resulting macroscopic electric field cannot be expressed as a function of the electronic density alone, the approach requires us to introduce polarization as an additional independent degree of freedom,[35,36] the gauge field $\mathbf{A}_{\mathrm{eff}}(\mathbf{r},t)$. Formally, this is achieved by a generalization of the effective one-electron Kohn-Sham scheme, where electrons move in time-dependent effective potentials $\{v_{\mathrm{eff}}(\mathbf{r},t),\mathbf{A}_{\mathrm{eff}}(\mathbf{r},t)\}$, which are uniquely determined (apart from an arbitrary gauge transform) by the exact time-dependent density and currents. Our implementation is based on the Lagrangian formalism proposed by Bertsch *et al.*,[14] with (dropping the subscript "eff" from the vector field, $\mathbf{A}_{\mathrm{eff}}$)

$$\begin{aligned}\mathcal{L}=\int_\Omega d\mathbf{r}\Bigg(&\sum_i^{N_e}\frac{1}{2}\psi_i^*(\mathbf{x})(\nabla/i+e\mathbf{A})^2\psi_i(\mathbf{x})-\frac{1}{8\pi}|\nabla\phi(\mathbf{x})|^2\\&-i\psi_i^*(\mathbf{x})\frac{\partial}{\partial t}\psi_i(\mathbf{x})-e\big(\rho(\mathbf{x})-\rho_{\mathrm{ion}}(\mathbf{x})\big)\phi(\mathbf{x})\\&+\int_\Omega d^3r'\mathcal{V}_{\mathrm{ion}}^{NL}\big(\rho(\mathbf{x},\mathbf{x}')\big)\Bigg)-\frac{\Omega}{8\pi}\left(\frac{d\mathbf{A}}{dt}\right)^2+E_{xc}[\rho(\mathbf{x})],\end{aligned} \tag{6}$$

where $\mathbf{x}=(\mathbf{r},t)$, $c=\hbar=m_e=1$, ψ_i are the KS states, ϕ is the periodic part of the external Coulomb potential, V_{ion}^{NL} is the gauged nonlocal part of the ionic pseudopotentials, $\mathcal{V}_{\mathrm{ion}}^{NL}(\rho(\mathbf{x},\mathbf{x}'))=V_{\mathrm{ion}}^{NL}(e^{ie\mathbf{A}(\mathbf{r}-\mathbf{r}')}\rho(\mathbf{x},\mathbf{x}'))$, E_{xc} is the DFT exchange and correlation energy functional, and Ω is the volume of the simulation box. The macroscopic electric field is then given by $\mathbf{E}=-\nabla\phi-\frac{d\mathbf{A}}{dt}$.

In the following application the system is perturbed by making a sudden change in $\mathbf{A}$, $\mathbf{A}(t_{0+})=\mathbf{A}_0$, along the z axis. The stationary principle applied to the Lagrangian leads to coupled equations of motion for the Kohn-Sham states[14,37]

$$\begin{aligned}i\frac{\partial}{\partial t}\psi_i(\mathbf{x})=&\frac{1}{2}[\nabla/i+e\hat{z}A(t)]^2-e\phi(\mathbf{x})\psi_i(\mathbf{x})\\&+\frac{\delta E_{xc}}{\delta\rho(\mathbf{x})}[\rho(\mathbf{x})]\psi_i(\mathbf{x})\\&+\int_\Omega d\mathbf{r}'e^{-ieA(t)z}\mathcal{V}_{\mathrm{ion}}^{NL}(\mathbf{r},\mathbf{r}')e^{ieA(t)z'}\psi_i(\mathbf{x}),\end{aligned} \tag{7}$$

the scalar potential $\phi(\mathbf{x})$,

$$\nabla^2\phi(\mathbf{x})=-4\pi[-e\rho(\mathbf{x})+e\rho_{\mathrm{ion}}(\mathbf{x})], \tag{8}$$

and the vector potential $A(t)$,

$$\frac{\Omega}{4\pi}\frac{d^2A(t)}{dt^2}=\Omega j_{\mathrm{mac}}(t), \tag{9}$$

where

$$j_{\mathrm{mac}}(t)=\sum_i\frac{-e}{\Omega}\int_\Omega d\mathbf{r}d\mathbf{r}'\psi_i^*(\mathbf{x})e^{-ieA(t)z}v_z(\mathbf{r},\mathbf{r}')e^{ieA(t)z'}\psi_i(\mathbf{x}) \tag{10}$$

is the macroscopic electric current density with

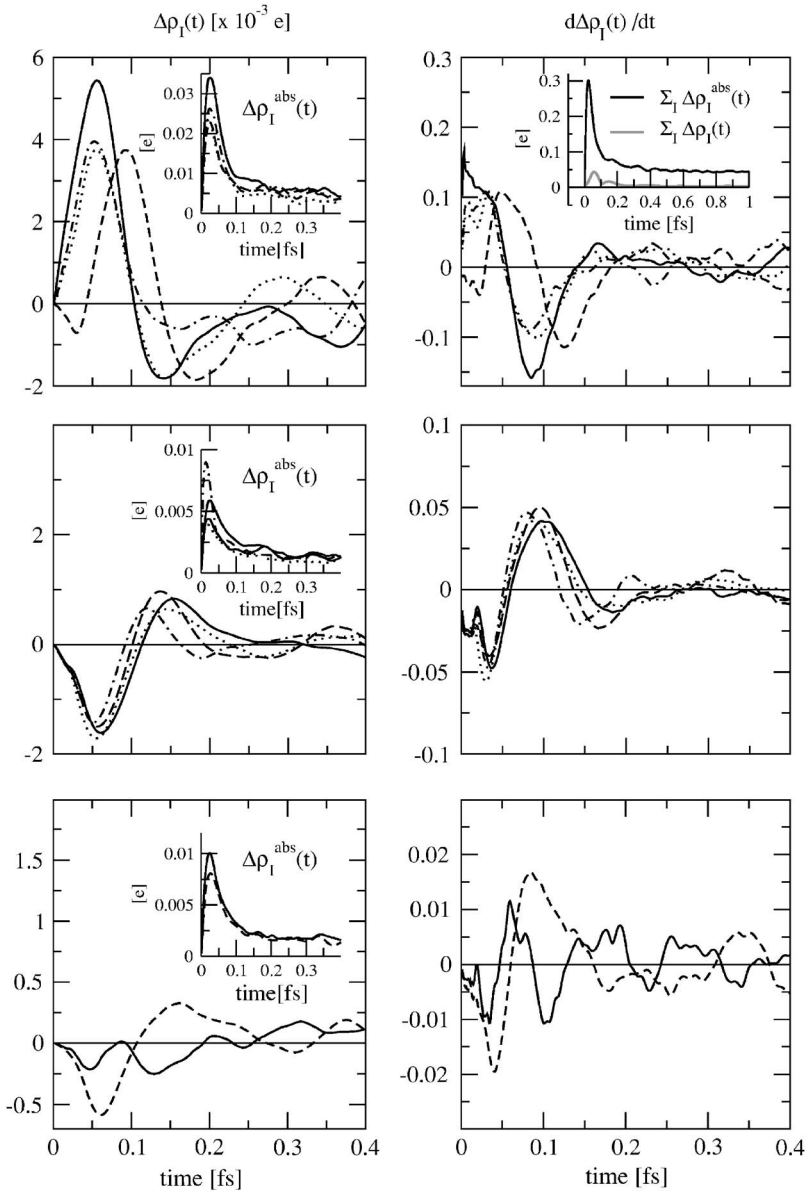

FIG. 1. Time series for the electron density fluctuations and currents corresponding to the volume elements Ω_I (see the text for a definition of the different quantities). Left column: The difference between the time evolution of $\Delta\rho_I(t)$ and $\Delta\rho_I^{\mathrm{abs}}(t)$ (insets) is a measure of the deviation from the Clausius-Mossotti limit. A selection of volume elements chosen according to their distance from the origin of the perturbation is shown: first (upper panel), second (middle panel), and third (lower panel) coordination sphere (different line styles indicate different representative molecules within the same coordination sphere). Right column: The currents between adjacent volume elements, $d\Delta\rho_I(t)/dt$, can be measured (same sequence as for the plots in the left column). In the inset of the upper plot, the total charge separation [sum over I=1,...,32 of the contributions $\Delta\rho_I(t)$] (gray) is compared with the total absolute charge separation (black).

$$v_z(\mathbf{r},\mathbf{r}') = (\nabla_z/i)\,\delta(\mathbf{r}-\mathbf{r}') + i\left[\mathcal{V}_{\mathrm{ion}}^{NL}(\mathbf{r},\mathbf{r}')z' - z\mathcal{V}_{\mathrm{ion}}^{NL}(\mathbf{r},\mathbf{r}')\right]. \tag{11}$$

III. POINT CHARGE PERTURBATION

The elementary density quantum in liquid water is the valence plasmon, which is believed to arise from collective oscillations of the $2s$ and $2p$ shells of the oxygen atoms at the characteristic frequency $\omega_p \simeq 22$ eV.[5,6] Since our computations only consider valence electrons of the oxygen atoms (together with the $1s$ electrons of the hydrogens), the quality of our results is strongly related to the validity of this assumption. In general, the electronic density of the sample should be regarded as a continuous function of the position, and single electrons cannot be assigned to individual water molecules of the system. In Fig. 1 we show the electron density fluctuations in Voronoi polyhedra constructed around the different water molecules after the perturbation induced by a sudden point charge of value $1e$ placed in the center of the simulation cell. We report the charge fluctuations and currents as a function of time for a few representative water molecules in the first, second, and third coordination spheres around the point of perturbation. Even if the relative orientation of the molecules inside the same shell differs, the oscillating dynamics of the quantities $\Delta\rho_I(t)=\int_{\Omega_I} d\mathbf{r}\,\delta\rho_I(\mathbf{r})$ (Fig. 1, left column) and $\Delta\rho_I^{\mathrm{abs}}(t)=\int_{\Omega_I} d\mathbf{r}|\delta\rho_I(\mathbf{r})|$ (inset) is coherent, which is an additional proof of the collective character of the response ($\delta\rho_I$ stands for the electron density difference computed for the Voronoi polyhedra centered at the water molecule I and with volume Ω_I). The average period of the first oscillation of $\Delta\rho_I(t)$ computed for the first shell of water molecules around the perturbation point amounts to $\sim$190 as, which corresponds to a plasmon frequency $\omega_p \simeq 21.7$ eV.

The dipole moment of the density of the constitutive elements is not a good measure of the polarization because currents can flow across the borders of the partitioning polyhe-

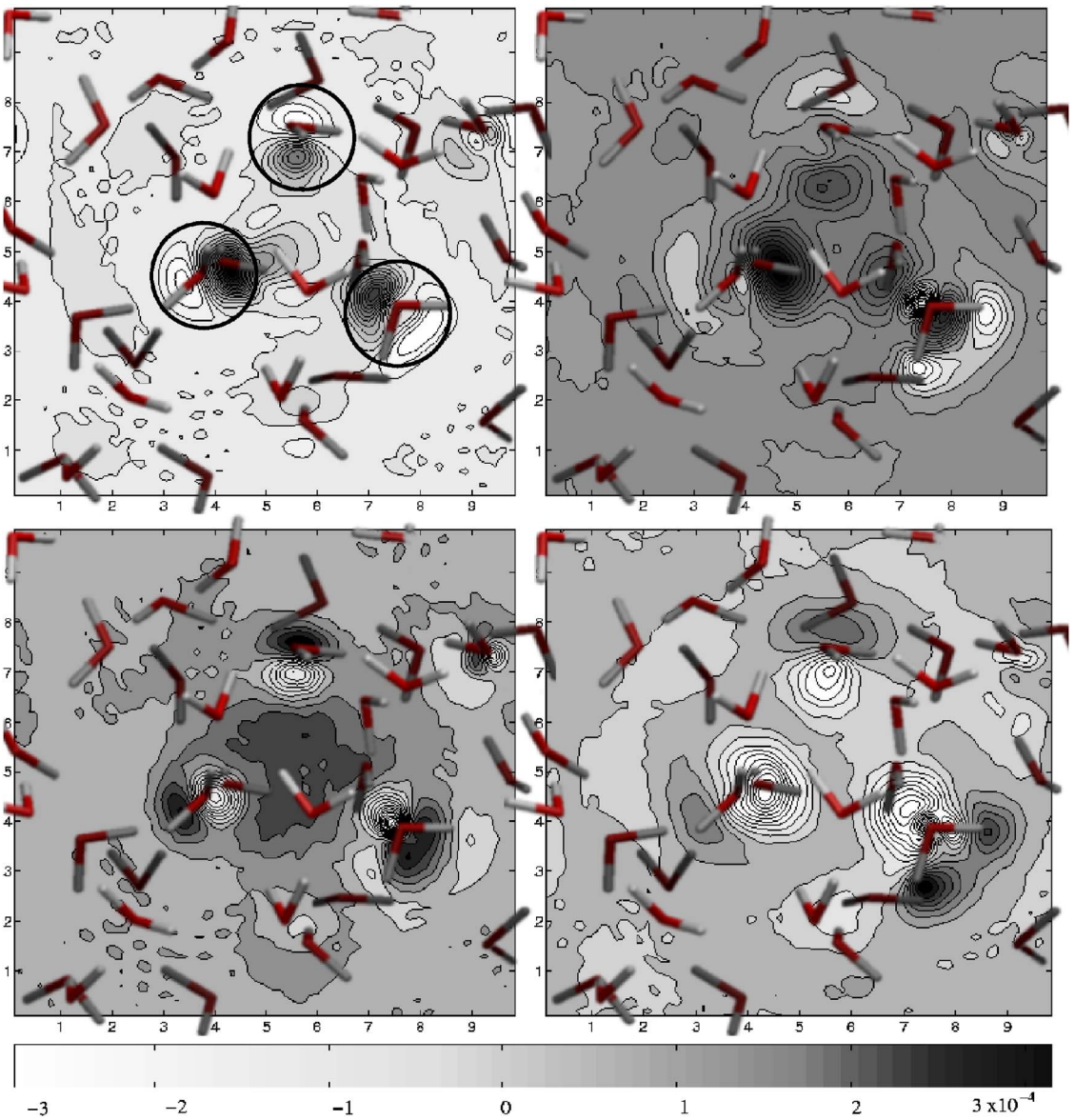

FIG. 2. (Color online) Two-dimensional density profiles for $\delta\rho(dt)=\rho(t_0)-\rho(t)$ after a sudden switch on of a point charge of $1e$ at the center of the box at time t_0. Positive (negative) values stand for an increase (depletion) of electronic density in units of e. From the top left corner, dt=35, 60, 85, and 120 as. The molecules close to the plane are marked by a dark circle.

dra. The computed currents through the boundaries of the different volumes Ω_I are shown in Fig. 1 (right column, from the top to the bottom) for the same collection of water molecules. In the inset (upper panel) we plot the time series for the total absolute density displacement $\Delta\rho^{\mathrm{abs}}(t)=\Sigma_{I=1}^{32}\Delta\rho_I^{\mathrm{abs}}(t)$ (black curve) and the total density displacement $\Delta\rho(t)=\Sigma_{I=1}^{32}\Delta\rho_I(t)$ (gray curve). After the initial fast recovery lasting a few attoseconds, the quantity $\Delta\rho^{\mathrm{abs}}(t)$ reaches an asymptotic value of $\sim 0.048e$. This fraction of density cannot recombine to give the initial equilibrium electron density distribution because it arises from the component of the electronic wave function excited into a higher energy level during the perturbation. The difference between the two curves gives a measure of the dipole oscillation (charge separation and recombination) inside a single volume element, while the area below the gray curve represents the component that flows between adjacent polyhedra. We have therefore a measure of the breakdown of the Clausius-Mossotti limit,[38] which describes the electronic response as the sum of neutral and independently polarizable entities.

Figure 2 displays four snapshots of the density difference $\delta\rho(\mathbf{r},t)=\rho_0(\mathbf{r})-\rho(\mathbf{r},t)$, which, in the case of a δ-type perturbation, corresponds to the response function $\tilde{\chi}(\mathbf{r},t)$.

Again, the perturbation is induced by a point charge of value $1e$ at the center of the box, and in Fig. 2 we show the contour plots of the density disturbance measured on a central plane at 35, 60, 85, and 120 as after t_0. Since the system is not isotropic, the disturbance is not spherically symmetric, unlike the case obtained under experimental conditions.[6] Nevertheless, it is possible to recognize a shell structure centered at the position of the disturbance (center of the box). At

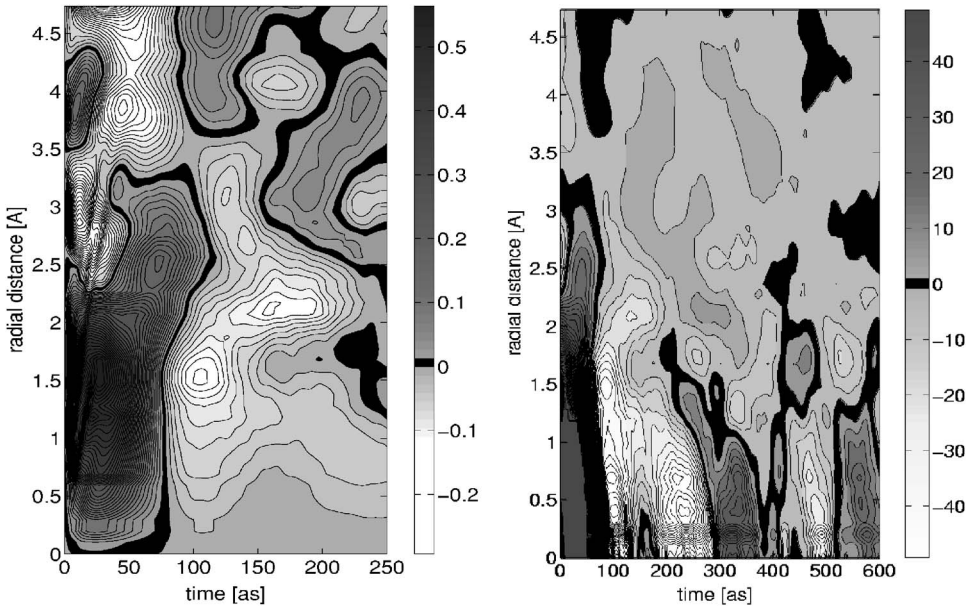

FIG. 3. Left panel: Radial distribution of the electronic disturbance, $\delta\rho_r(t)=r^2\int d\Omega_r \delta\rho(\mathbf{r},t)$ within a spherical shell of thickness dr and radius r, during the first 200 as after perturbation. The displacement of the peaks during the first relaxation period (~80 as) occurs at a speed of ~0.035 Å/as. (Dark gray: excess electron density; light gray: electron "hole". The contour at 0 is shown in black.) Right panel: Corresponding radial density distribution, $\delta\tilde{\rho}_r(t)=\delta\rho_r(t)/(4\pi r^2 dr/\Omega)$. The oscillation of the electronic disturbance, $\tilde{\rho}_r(t)$, close to the center of the box, $r=0$, occurs at a frequency $\omega_p \simeq 21.75$ eV.

each shell, the maximum of the function $\tilde{\chi}(|\mathbf{r}|,t)$ is picked close to the position of the oxygen and hydrogen atoms, but we also observe an intermolecular component, which is particulary important in the very short time interval following the perturbation. After 12 as, the excess charge density within a sphere of ~1 Å radius at the box center amounts to $\sim 0.15e$ and is not centered on any molecule. The lifetime of this state is, however, very short. After 95 as the perturbation has inverted its sign, with a positive charge (hole) at the center of the box and the negative charge moved to an outer concentric shell.

The dimensions of the propagating disturbance and its dynamics, shown in Fig. 3, are in qualitatively good agreement with the experimental data for a corresponding isotropic medium.[6] The left panel of Fig. 3 shows the time evolution of the radial disturbance, $\delta\rho_r(t)=r^2\int d\Omega_r \delta\rho(\mathbf{r},t)$ during the first 200 as following the perturbation, and gives an estimate of the initial radial propagation speed of the perturbation (~0.035 Å/as). After the first 50 as, the electronic disturbance localizes at a distance within 4 Å from the origin of the δ pulse. As the system approaches the thermal equilibrium, we observe a damping of the perturbation amplitude. This is in agreement with the experimental observation that a plasmon in water never develops into a time-propagating mode.[6] The radial density distribution of $\delta\rho_r(t)$, $\delta\tilde{\rho}_r(t)=\delta\rho_r(t)/(4\pi r^2 dr/\Omega)$, over a period of 600 as is shown in the right panel of Fig. 3. The first three complete (an)harmonic oscillation cycles of the electronic disturbance, $\tilde{\rho}_r(t)$, close to the center of the box ($r=0$) occur within the initial 580 as of dynamics and correspond to a period T_p of ~193 as, which is again in agreement with the time scale of a plasmon oscillation, $\omega_p=2\pi/T_p \simeq 21.75$ eV.

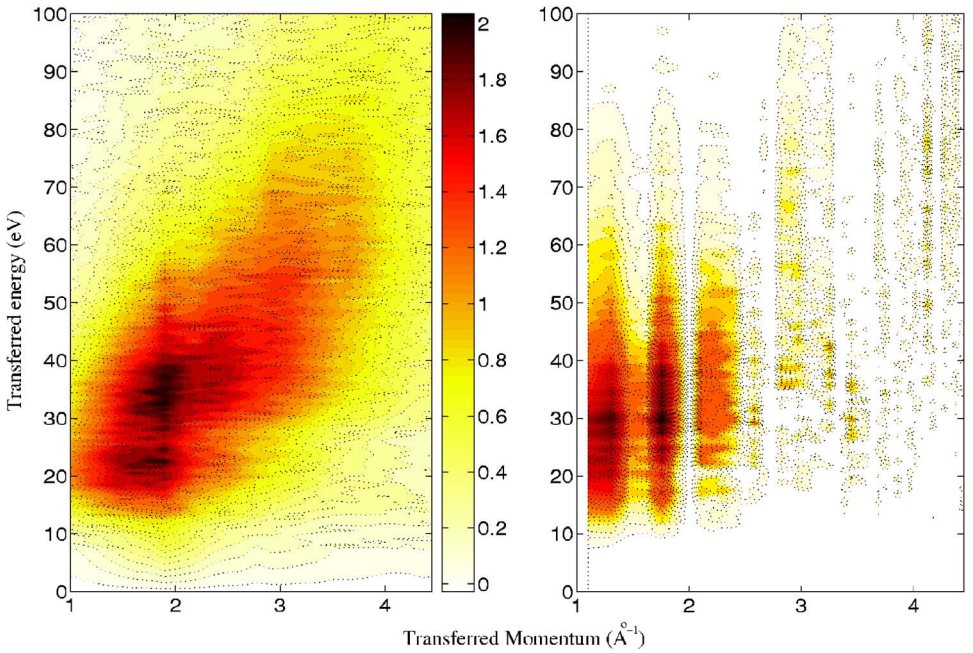

FIG. 4. (Color online) Left: False color plot of $-\mathrm{Im}\,\tilde{\chi}(\mathbf{k},\omega)$ of water in units of as/Å^3 plotted against transferred momentum (x-ray experimental data from Ref. 6). Right: Same function computed for two equilibrated frames. Data are collected every 1.2 as for a total length of 4 fs. The color code is arbitrary and is chosen to match the experimental values. The shell structure in k-space sampling is a consequence of the finite size of the simulation cell.

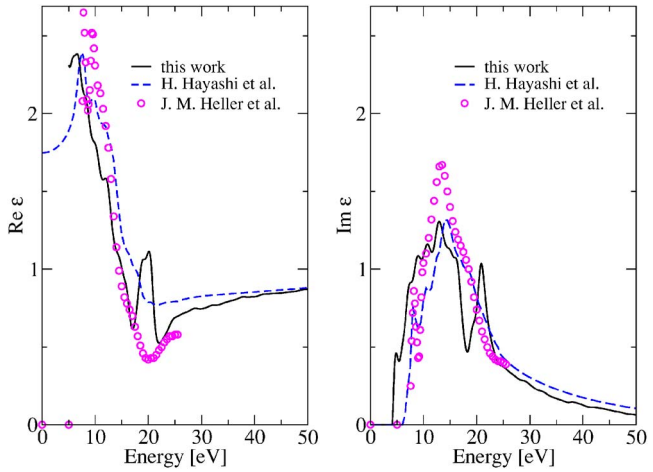

FIG. 5. (Color online) Real and imaginary parts of the dielectric function of liquid water. For comparison experimental data from Hayashi *et al.*[5] (dashed curves) and Heller *et al.*[4] (symbols) are also shown.

The use of a plane wave basis set allows the direct computation of the response function $\tilde{\chi}(\mathbf{k},t)$ in Fourier space. The advantage of this description lies in the simple interpretation of $\tilde{\chi}$ as a density propagator, which describes the dynamics of the disturbance in the electron density in terms of plane waves with momenta k and energy $\hbar\omega$. As mentioned before, the anisotropy of the sample makes the choice of this basis set less natural. However, an average over different structures would lead to a result comparable to experiments. Figure 4 shows a comparison of the computed imaginary part of the response function, $-\mathrm{Im}\,\tilde{\chi}(\mathbf{k},\omega)$, with the results from Ref. 6. The transferred momenta $\mathbf{k}$ was sampled at a $\Delta k = 0.3373$ Bohr^{-1}. The discreteness of the sampling in the reciprocal k space is responsible for the discontinuities along the abscissa.

IV. DIELECTRIC FUNCTION

Using the real-space real-time method[14] for the simulation of the response induced by the action of an external constant electric field pulse, $E_z(t)=-A_0\delta(t)$ along the z axis ($A_0=5\times10^6$ V/m), we computed the dielectric function for two liquid water configurations obtained from a preparatory run at 298 K. The polarization electric field, $E_z(t)=-dA(t)/dt$, can be used to compute the dielectric function according to Eq. (2) ($\eta=0.001$ eV). This result is shown in Fig. 5 for the real and imaginary parts of the dielectric response function together with experimental x-ray values from Hayashi *et al.*[5] and Heller *et al.*[4]

The overall agreement between the three sets of data is remarkable, especially if we consider the small size of the unit cell used in the calculations and the limited sampling. Experimentally, the plasmon frequency is measured at 22 eV,[5,6] while from the peak in $-\mathrm{Im}(\epsilon^{-1}(\omega))$ we obtained a value of 21.6 eV. The position of the maximum of $-\mathrm{Im}\,\varepsilon(\omega)$ and its value are also in good agreement with the measurements of Hayashi and co-workers.[5]

V. CONCLUSIONS

In conclusion, we have successfully computed the electronic response properties of liquid water using a real-time propagation scheme for the solution of the time-dependent Kohn-Sham equations in the presence of an external perturbation. For this purpose, we have used two different perturbations schemes, namely a point charge disturbance and a sudden switch of an external constant electric field.

We found a good agreement between the computed response properties of a sample made of 32 water molecules and the experimental values measured in liquid water. The investigated quantities include the dielectric function, the plasmon frequency, and the linear response function in k space. In addition, the method has allowed, for the first time, the characterization of electronic density oscillations, their spatial amplitude, and temporal decay, at an atomistic scale and with a time resolution in attoseconds.

This approach, implemented within the so-called adiabatic approximation, combines computational efficiency and accuracy and is therefore suited for the *ab initio* study of the electronic response properties of complex molecular systems such as liquids. In the case of disordered systems, the equilibration of the sample constitutes an important step in the analysis and requires the same level of accuracy used for the response calculation. In this study we took advantage of the long experience accumulated over the last decades in the study of the structural and electronic properties of liquid water described within DFT.[39]

ACKNOWLEDGMENTS

The author thank G. F. Bertsch and K. Yabana for the help with the real-time propagation scheme. We also acknowledge P. Abbamonte for the experimental data reported in Fig. 4, C.-C. Kao, H. Hayashi, and M. Dingfelder for the data of Fig. 5, and U. Röthlisberger, M. Sprik, and R. Resta for discussions.

[1] Ph. Wernet *et al.*, Science **304**, 995 (2004).
[2] J. D. Smith *et al.*, Science **306**, 851 (2004).
[3] P. L. Silvestrelli and M. Parrinello, J. Chem. Phys. **111**, 3572 (1999).
[4] J. M. Heller, R. N. Hamm, R. D. Birkhoff, and L. R. Painter, J. Chem. Phys. **60**, 3483 (1974).
[5] H. Hayashi, N. Watanabe, Y. Udagawa, and C. C. Kao, Proc. Natl. Acad. Sci. U.S.A. **97**, 6264 (2000).
[6] P. Abbamonte, K. D. Finkelstein, M. D. Collins, and S. M. Gruner, Phys. Rev. Lett. **92**, 237401 (2004).
[7] G. D. Kerr, R. N. Hamm, M. W. Williams, R. D. Birkhoff, and L. R. Painter, Phys. Rev. A **5**, 2523 (1972).

[8] M. Dingfelder, D. Hantke, M. Iokuti, and H. G. Paretzke, Radiat. Phys. Chem. **53**, 1 (1998).
[9] W. E. Wilson and H. Nikjoo, Radiat. Environ. Biophys. **38**, 97 (1999).
[10] L. Bernasconi, M. Sprik, and J. Hutter, J. Chem. Phys. **119**, 12417 (2003).
[11] A. Selloni, P. Carnesvali, R. Car, and M. Parrinello, Phys. Rev. Lett. **59**, 823 (1987).
[12] M. Boero, M. Parrinello, K. Terakura, T. Ikeshoji, and C. C. Liew, Phys. Rev. Lett. **90**, 226403 (2003).
[13] A. L. Fetter and J. D. Walecka, *Quantum Theory of Many-Particle Systems* (McGraw-Hill, Inc., New York, 1971).
[14] G. F. Bertsch, J.-I. Iwata, A. Rubio, and K. Yabana, Phys. Rev. B **62**, 7998 (2000).
[15] E. Runge and E. K. U. Gross, Phys. Rev. Lett. **52**, 997 (1984).
[16] M. E. Casida, in *Recent Developments and Applications of Modern Density Functional Theory*, edited by J. M. Seminario (Elsevier, Amsterdam, 1996), Vol. 4.
[17] E. K. U. Gross, J. F. Dobson, and M. Petersilka, in *Density Functional Theory*, edited by R. F. Nalewajski, Springer Series in Topics in Current Chemistry (Springer, New York, 1996), Vol. 181.
[18] G. Onida, L. Reining, and A. Rubio, Rev. Mod. Phys. **74**, 601 (2002).
[19] S. J. A. van Gisgergen, P. R. T. Schipper, O. V. Gritsenko, E. J. Baerends, J. G. Snijders, B. Champagne, and B. Kirtman, Phys. Rev. Lett. **83**, 694 (1999).
[20] I. Tavernelli, U. F. Röhrig, and U. Rothlisberger, Mol. Phys. **103**, 963 (2005).
[21] K. Burke, J. Werschnik, and E. Gross, J. Chem. Phys. **123**, 062206 (2005).
[22] K. Yabana and G. F. Bertsch, Phys. Rev. B **54**, 4484 (1996).
[23] A. Castro, M. A. L. Marques, and A. Rubio, J. Chem. Phys. **121**, 3425 (2004).
[24] R. van Leeuwen, Phys. Rev. Lett. **80**, 1280 (1998).
[25] R. Baer and R. Gould, J. Chem. Phys. **114**, 3385 (2001).
[26] J. Theilhaber, Phys. Rev. B **46**, 12990 (1992).
[27] J. Hutter *et al.*, *CPMD, version 3.8*, Copyright IBM Corp. 1990–2001, Copyright MPI-FKF Stuttgart 1997-2005, http://www.cpmd.org.
[28] N. Troullier and J. L. Martins, Phys. Rev. B **43**, 1993 (1991).
[29] L. Kleinman and D. M. Bylander, Phys. Rev. Lett. **48**, 1425 (1982).
[30] A. D. Becke, Phys. Rev. A **38**, 3098 (1988).
[31] C. Lee, W. Yang, and R. G. Parr, Phys. Rev. B **37**, 785 (1988).
[32] E. K. U. Gross and W. Kohn, Adv. Quantum Chem. **21**, 255 (1990).
[33] R. Car and M. Parrinello, Phys. Rev. Lett. **55**, 2471 (1985).
[34] S. Nosé and M. L. Klein, Mol. Phys. **50**, 1055 (1983); S. Nosé, *ibid.* **52**, 255 (1984); W. G. Hoover, Phys. Rev. A **31**, 1695 (1985).
[35] S. K. Ghosh and A. K. Dhara, Phys. Rev. A **38**, 1149 (1988).
[36] X. Gonze, P. Ghosez, and R. W. Godby, Phys. Rev. Lett. **74**, 4035 (1995).
[37] K. Yabana, private communication.
[38] J. D. Jackson, *Classical Electrodynamics* (J. Wiley and Sons, New York, 1962).
[39] J. VandeVondele, F. Mohamed, M. Krack, J. Hutter, M. Sprik, and M. Parrinello, J. Chem. Phys. **122**, 014515 (2005).